

PAPER • OPEN ACCESS

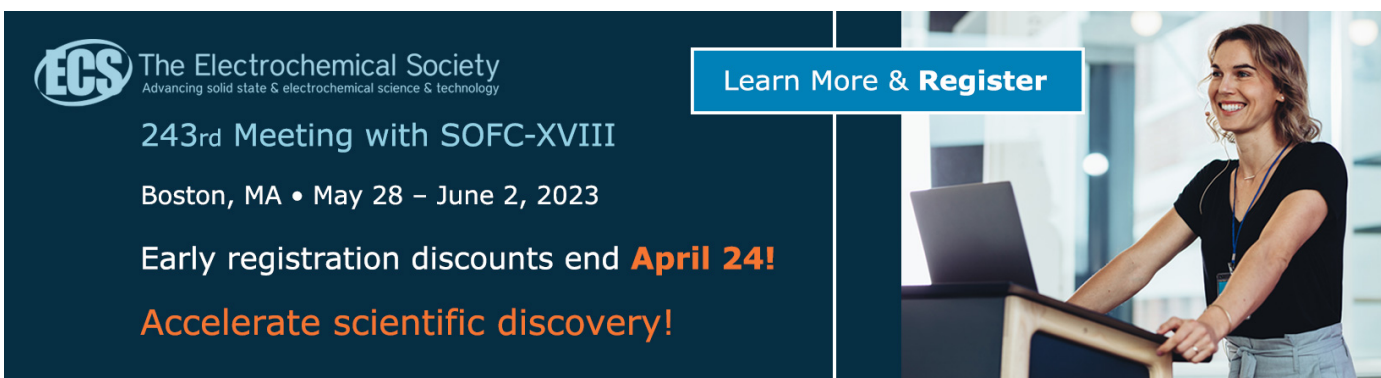
## Synthesis of nano-crystalline forsterite based on amorphous silica powder from natural sand by mechanical activation method

To cite this article: U Nurbaiti *et al* 2019 *J. Phys.: Conf. Ser.* **1170** 012069

View the [article online](#) for updates and enhancements.

You may also like

- [Patchy Forsterite Clouds in the Atmospheres of Two Highly Variable Exoplanet Analogs](#)  
Johanna M. Vos, Ben Burningham, Jacqueline K. Faherty et al.
- [Corrosion evaluation of nanocomposite gelatin-forsterite coating applied on AISI 316 L stainless steel](#)  
Mohammed T Hayajneh, Mohammed A Almomani and Heba B Al\_hmoud
- [CRYSTALLOGRAPHICALLY ANISOTROPIC SHAPE OF FORSTERITE: NEW PROBE FOR EVALUATING DUST FORMATION HISTORY FROM INFRARED SPECTROSCOPY](#)  
Aki Takigawa and Shogo Tachibana




**ECS** The Electrochemical Society  
Advancing solid state & electrochemical science & technology

243rd Meeting with SOFC-XVIII  
Boston, MA • May 28 – June 2, 2023

Early registration discounts end **April 24!**  
**Accelerate scientific discovery!**

Learn More & Register



# Synthesis of nano-crystalline forsterite based on amorphous silica powder from natural sand by mechanical activation method

U Nurbaiti<sup>1,\*</sup>, A Kholifatunnisa<sup>2</sup> and S Pratapa<sup>2</sup>

<sup>1</sup> Physics Department, Universitas Negeri Semarang, Jl. Raya Sekaran Gunungpati, Semarang 50221, Indonesia

<sup>2</sup> Physics Department, Institut Teknologi Sepuluh Nopember Surabaya, Jl. Arief Rahman Hakim, Surabaya 60111, Indonesia

\*Corresponding author: upik\_nurbaiti@mail.unnes.ac.id

**Abstract.** The synthesis of nano-forsterite powders has been succeeded using an amorphous SiO<sub>2</sub> powder base material from the purification of natural silica sands from Tanah Laut and MgO Merck with a combination of duration of mechanical activation and calcination temperature. The silica and magnesia powders are mixed and mechanically activated using ball mill for 1, 2, 3 hours. The mixture was then calcined at a temperature of 950, 1050, and 1150°C for 4 hours to form a forsterite powder. Phase characterization was performed using X-Ray Diffraction (XRD), while the crystalline size using Transmission Electron Microscopy (TEM). The analysis of diffraction data was done using the Rietica software method. Overall the phases formed after calcination are forsterite, periclase, cristobalite, and protoenstatite. The highest percentage of forsterite weight was obtained in the sample with a 3-hour mechanical activation treatment with a calcination temperature of 950 °C, i.e. 87.9 wt. At all temperatures, the forsterite content increases with increasing time of mechanical activation. An important invention in this study, when compared with earlier literature, is that high concentrations of forsterite can be formed at lower calcination temperatures. Observations with TEM show that the size of forsterite crystals is reduced along with the increase in the time of mechanical activation. The size of the forsterite crystals in the calcined samples of 950° C after mechanical activation for 3 hours was about 81 nm, whereas in the calcined samples 1050 °C without mechanical activation about 94 nm.

## 1. Introduction

Forsterite (Mg<sub>2</sub>SiO<sub>4</sub>) is a crystalline silicate with an orthorhombic crystal system [1] and a Pbnm space group. Forsterite is also composed of SiO<sub>4</sub><sup>-4</sup> anions and Mg<sup>2+</sup> cations with a 1: 2 molar choice [2]. The advantages of forsterite have low electrical conductivity, small dielectric constants ( $\epsilon_r = 6.8$ ) [3], chemically stable [4], good electrical insulation (electrical resistance ~1013-1015  $\Omega\text{cm}$ ) [5], and melting point 1890 °C [6]. Therefore, Forsterite is a material potentially to be applied to various areas of life.

Some forsterite applications in the advent technology are used as a dielectric for millimeter waves [7] and insulator material for Solid Oxide Fuel Cell (SOFC) because it has a good thermal expansion coefficient and high stability [8]. In the field of medical forsterite is used for tissue engineering applications [9,10], radiotherapy [11], and as bone implants [12]. Therefore, some efforts are made to produce forsterite with high purity, both regarding basic materials and methods of manufacture.



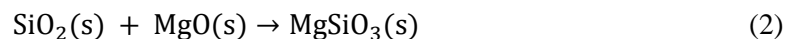
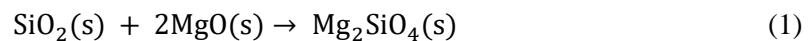
Several methods have been carried out on the synthesis of forsterite among which are sol-gel [13], coprecipitation [14], solid reaction [12] and mechanical activation [1,15]. Although Fathi and Kharaziha [1] have performed forsterite synthesis with mechanical activation, the basic ingredients used are magnesium carbonate ( $\text{MgCO}_3$ ) and amorphous  $\text{SiO}_2$ . Tavangarian and Emadi [3] have also performed forsterite synthesis with mechanical activation using talc base material ( $\text{Mg}_3\text{Si}_4\text{O}_{10}(\text{OH})_2$ ) and magnesium carbonate ( $\text{MgCO}_3$ ). The results of the research are claimed to have high purity forsterite, milling time of more than 10 hours, high calcination temperature ( $>1200^\circ\text{C}$ ) and the purity percentage quantity is not specified. It is, therefore, necessary to make a breakthrough by enriching the raw material to empower the potential around us given that forsterite can be synthesized from precursors containing silica oxide and magnesium oxide. The amorphous silica base material (ATL) purified from the silica sand as a source of the silica oxide was successful synthesis to form nano-forsterite powder by mechanical activation method [16], but the periclase was still encountered (~11 wt%). Therefore, it is urgent to reduce MgO composition on starting materials to remove the appearance of periclase as a secondary phase. This paper reports the influence of the milling time (1, 2 and 3h) at various low calcination temperature (950, 1050 and  $1150^\circ\text{C}$ ) to the purity of forsterite.

## 2. Methods

ATL and MgO powder were weighed using a digital balance sheet with a composition of 49.2 wt%  $\text{SiO}_2$  and 50.8 wt% MgO, a preformed composition approximating a 1: 2 mol ratio of stoichiometry between  $\text{SiO}_2$  and MgO, then added 3wt% PVA of the total weight of  $\text{SiO}_2$  and MgO. Here, PVA acts as an additive. The mixing process is carried out with or without mechanical activation. The process without mechanical activation is done by mortar. Mechanical activation is carried out for 1, 2, and 3 hours. Then in each sample calcination was done at temperature 950, 1050, and  $1150^\circ\text{C}$  for 4 hours holding time. There are 12 samples with FTL 950-1150 0-3 nomenclature, code number hundreds and thousands of letters behind the significance of the calcination temperature while the number of units that follow behind means the time of milling. All the calcined samples were then tested by X-ray diffraction (XRD) for phase composition analysis, whereas for grain size analysis only 2 samples were selected in the TEM test.

## 3. Result and Discussion

Figure 1 presents the diffraction patterns of all synthesized samples showing that forsterite has been formed at all calcination temperatures with or without mechanical activation. Sanosh et al. [13] state that forsterite begins to form at a temperature of  $800^\circ\text{C}$ . Despite the stoichiometric ideal 1:2 molarity ratio, the forsterite phase formed is always followed by secondary phases. The presence of secondary phase is caused because forsterite can also be formed because of the reaction between MgO on the surface of  $\text{SiO}_2$  to form the enstatite, so it is natural that the enstatite phase ( $\text{MgSiO}_3$ ) or polymorphic (proto-enstatite and clinoenstatite) occurs. After that, the forsterite formation phase can continue when there is excess MgO diffusing through the surface of the enstatite [17]. So the mechanism of the formation reaction of forsterite in this study can be formulated in the following equation:



XRD data for FTL 950 3 samples showed fairly wide forsterite peaks and indicated the formation of nano-forsterite. To confirm this formation, observations were made with TEM. Based on the TEM image in Fig. 2 it can be estimated that the distribution of crystal size in FTL 950 3 and FTL 1050 0 samples is approximately 81 nm and 94 nm, respectively. The increasing of the crystal size as shown in Fig. 2 (B) is due to the higher calcination temperature so that grain growth is increasing. On the other hand in Fig. 1A, mechanical activation is carried out for 3 hours and calcined at a lower temperature so that the crystal size is smaller. Thus the purpose of the mechanical activation has been achieved that is to increase the reactivity so that the desired phase can be formed at a lower calcination temperature. The formation of the phase is due to the increased diffusion rate and the homogeneity of the particles.

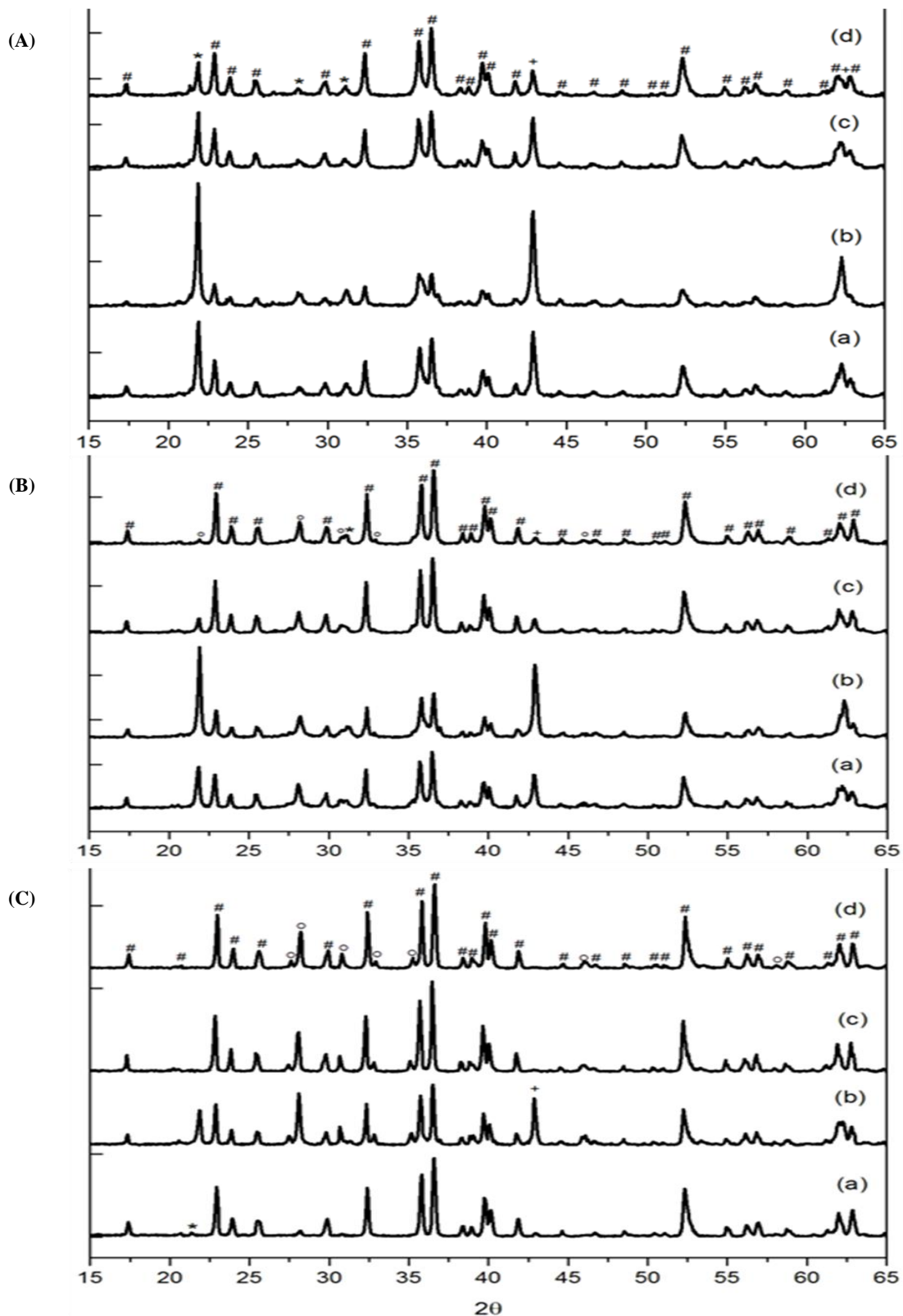


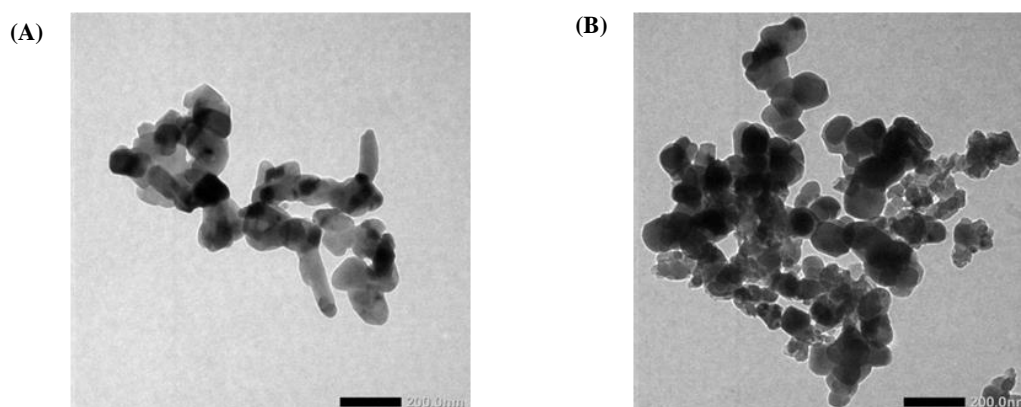
**Figure 1.** X-Ray Diffraction Patterns (CuK $\alpha$  radiation) of Samples after Calcined at (A) 950, (B) 1050 and (C) 1150°C for Mechanical Activation (a) 0, (b) 1, (c) 2 and (d) 3 h. The indexed peaks: # = Forsterite, + = Periclase, \* = Cristobalite and o = Protoenstatite

**Table 1.** The percentage of the weight of the phase formed in each sample was calculated using Rietica software by the Ritveld method.

Sample	% Berat			
	Forsterit	Periklas	Kristobalit-Low	Protoenstatit
FTL 950 0	66,9	23,6	9,5	-
FTL 1050 0	64,4	11,2	4,5	19,9
FTL 1150 0	94,8	1,4	0,4	3,4
FTL 950 1	42,1	40,3	17,6	-
FTL 1050 1	48,3	24,9	8,9	17,9
FTL 1150 1	80,8	0,7	-	18,5
FTL 950 2	75,9	17,4	6,7	-
FTL 1050 2	77,4	5,9	1,3	15,4
FTL 1150 2	81,0	0,8	-	18,2
FTL 950 3	87,9	6,4	5,7	-
FTL 1050 3	80,4	2,3	0,5	16,8
FTL 1150 3	82,3	-	-	17,7

The forsterite phases ( $\text{Mg}_2\text{SiO}_4$ , PDF# 34-0189) and other phases identified are periclase ( $\text{MgO}$ , PDF# 45-0946), cristobalite-low ( $\text{SiO}_2$ , PDF# 82-1232) and proto-enstatite ( $\text{MgSiO}_3$ , PDF# 74-816) as shown in Table 1. Cristobalite is a  $\text{SiO}_2$  polymorph, and proto-enstatite is  $\text{MgSiO}_3$  polymorph. The presence of  $\text{SiO}_2$  and  $\text{MgO}$  indicates that the reaction between the two compounds is not yet perfect overall. Two things that are suspected to be the cause of the non-reaction of the two compounds are (1) the homogeneity of the second particle distribution of the compound and (2) the unavailability of energy for the reaction as in equation 1 as a result of the too low calcination temperature used. Meanwhile,  $\text{SiO}_2$  and  $\text{MgO}$  can react to form  $\text{MgSiO}_3$  according to equation 2 with several structures, one of which is proto-enstatite. This phase is formed at a temperature of calcination above  $1000^\circ\text{C}$  (Fig. 1B and 1C) as uncovered by Foster [18].

Based on the results obtained from the smoothing by using Rietica, each temperature increase at the same mechanical activation time, the forsterite content tends to rise, except for samples with a 3-hour mechanical activation time. The increase in percentage weight of the forsterite is due to the increasing availability of energy for the reaction along with the increasing temperature of calcination. The weight percentage decrease occurs when mechanical activation is 1 hour compared with no mechanical activation at all calcination temperatures.  $\text{MgO}$  and  $\text{SiO}_2$  have not fully reacted due to the inhomogeneity of particle distribution. Therefore, it can be said that the homogeneity of the particles in the sample without mechanical activation is better than the sample with 1-hour mechanical activation.

**Figure 2.** TEM image on samples (A) FTL 950 3 and (B) FTL 1050 0

At each temperature, the forsterite content always increases with the addition of mechanical activation time. The increase in percentage weight of the forsterite is due to changes in grain size, so homogeneity becomes better and more comfortable to react. The decrease in proto-enstatite and periclase content and increased forsterite with increasing mechanical activation time indicate the reaction between periclase and proto-enstatite according to equation 2 and equation 3. MgO reacts with SiO<sub>2</sub> to form the enstatite, then MgO diffuses on the enstatite to form the forsterite as disclosed by Brindley and Hayami [17].

The highest forsterite content with mechanical activation is the treatment of mechanical activation of 3 hours with a calcination temperature of 950 ° C that reaches 87.9% wt. The high percentage of weight in the treatment was due to improved homogeneity and proto-enstatite phase as well as mechanical activation with a temperature of calcination of 1050 and 1150°C which formed the proto-enstatite phase of 16.8 and 17.7wt% respectively. The highest forsterite content of the entire sample was in the treatment without mechanical activation with a temperature of calcination of 1150°C which reached 94.8wt%. This result is more effective than that obtained by [1] which is optimum when its mechanical activation for 10 hours with a calcination temperature of 1200°C. Especially when compared with the results obtained by [3] that produce forsterite with high purity after being treated with 100 hours of mechanical activation with a temperature of calcination 1200°C. Although in [7] improved the results of forsterite synthesis by mechanical activation using the same basic ingredients. The second study optimally resulted in forsterite in 60-hour mechanical activation treatment with a 1000 °C calcining temperature. While there is a marked improvement in the quality of milling time and calcination temperature, the research is considered never before to be effective and efficient regarding forsterite production.

#### 4. Conclusion

Success in synthesizing nano-forsterite with a fairly high percentage of weight (above 80wt%) although calcined at relatively low temperatures (below 1000°C) in this study. The treatment of mechanical activation time together with the calcination temperature in the fabrication process greatly influences the percentage of the purities of forsterite formed. Increased mechanical activation time in addition to increased the percentage of forsterite, it also decreases the calcination temperature and decreases the size of the crystals. The highest percentage of forsterite weight in the sample with mechanical activation was formed at 3-hour mechanical activation with a calcination temperature of 950°C, of 87.9wt%. Distribution of crystal size in samples with mechanical activation for 3 hours with a calcination temperature of 950°C and a sample without mechanical activation with a calcination temperature of 1050°C of approximately 81 nm and 94 nm.

#### Acknowledgments

The authors would like to thank DITJEN DIKTI for the cost assistance of the Superior Research Scheme of Higher Education 2015/2016 and Research Grant of Doctoral Dissertation 2017.

#### References

- [1] Fathi M H and Kharaziha M 2008 *Mater Lett* **62** 4306
- [2] Rani A B, Annamalai A R, Majhi M R and Kumar A H 2014 *Int J Chem Tech Res CODEN* **6** 1390
- [3] Tavangarian F and Emadi R 2009 *J Alloys Compd* **485** 648
- [4] Saberi A, Alinejad B, Negahdari Z, Kazemi F and Almasi A 2007 *Mater Res Bull* **42** 666
- [5] Sasikala T S, Suma M N, Mohanan P, Pavithran C and Sebastian M T 2008 *J Alloys Compd* **461** 555
- [6] Lin L, Yin M, Shi C and Zhang W 2008 *J Alloys Compd* **455** 327
- [7] Tavangarian F and Emadi R 2011 *Mater Lett* **65** 740
- [8] Kosanović C, Stubičar N, Tomašić N, Bermanec V and Stubičar M 2005 *J Alloys Compd* **389** 306
- [9] Diba M, Kharaziha M, Fathi M H, Gholipourmalekabadi M and Samadikuchaksaraei A 2012 *Compos Sci Technol* **72** 716

- [10] Yazdanpanah A, Kamalian R, Moztarzadeh F, Mozafari M, Ravarian R and Tayebi L 2012 *Ceram Int* **38** 5007
- [11] Cheng T W, Ding Y C and Chiu J P 2002 *Miner Eng* **15** 271
- [12] Ramesh S, Yaghoubi A, Lee K Y S, Chin K M C, Purbolaksono J, Hamdi M and Hassan M A 2013 *J Mech Behav Biomed Mater* **25** 63
- [13] Sanosh K P, Balakrishnan A, Francis L and Kim T N 2010 *J Alloys Compd* **495** 113
- [14] Wahsh M M S, Khattab R M, Khalil N M, Gouraud F, Huger M and Chotard T 2014 *Mater Des* **53** 561
- [15] Tavangarian F and Emadi R 2010 *Mater Res Bull* **45** 388
- [16] Nurbaiti U, Darminto, Triwikantoro, Zainuri M and Pratapa S 2018 *Ceram Int* **44** 5543
- [17] Brindley G W and Hayami R 1965 *Mineral Mag* **35** 189
- [18] Foster W R 1951 *J Am Ceram Soc* **34** 255